Frequency Fusion for Spread-Spectrum-Induced-Polarization Data Processing

Yao Hongchun[1], Guo Zhenwei[1,3] , Chen Rujun*[1], He Lanfang[4], Wu Yan[1] , Yang Shangyi[2]
1 Central South University, yhc511025@163.com
2 Giant Sequoia Artificial Intelligence Technology (Changsha) Co., Ltd., shangyi_yang@foxmail.com
3 Hunan Key Laboratory of Nonferrous Resources and Geological Hazards Exploration, guozhenwei@csu.edu.cn
4 Institute of Geology and Geophysics, Chinese Academy of Sciences, mofoo@263.net

SUMMARY

Induced Polarization (IP) method, which can measure both resistivity and chargeability, is widely used in the exploration of metal ore deposits. Addressing the issues of weak anti-interference capability and difficulty in distinguishing between ore and non-ore IP anomaly with conventional IP methods, we propose and implement a spread spectrum IP (SSIP) data processing method. This method utilizes the rich fundamental frequency components of pseudo-random spread spectrum signals to distinguish IP anomalies between ore and non-ore zones and employs a frequency fusion method to improve the anti-interference capability of IP parameters. Finally, field-measured data were used for processing tests. The results show that frequency fusion can enhance the anti-interference capability of IP parameters and allow for the adjustment of the number of frequencies fused according to the level of interference, ensuring the distinction of IP anomalies between ore and non-ore zones while maintaining data quality.

Keywords: Induced Polarization (IP); Spread Spectrum Signal; Frequency Fusion; Anomaly Differentiation

INTRODUCTION

The Induced Polarization (IP) method is an electrical exploration technique that utilizes the charge-discharge effect of rocks and minerals under electrical excitation to detect targets. This method can simultaneously measure resistivity and chargeability parameters, which are directly related to metal ore bodies and mineralization characteristics. It is currently considered the most promising geophysical method for metal ore exploration (Revil et al., 2022; Okada et al., 2022; Guo et al., 2020). However, with the increasing exploration depth and changing electromagnetic interference environments, conventional IP methods are facing issues such as weak anti-interference capabilities and difficulties in distinguishing between ore and non-ore IP anomalies, making it challenging to meet exploration needs. To address these issues, researchers have adopted methods such as combined techniques and multi-parameter fusion for metal ore identification (Su et al., 2023) and have utilized techniques like empirical mode decomposition and correlation analysis for noise reduction (Liu et al., 2019; Cen et al., 2023), but these methods still have various limitations.

To address these issues, we have proposed and implemented a spread spectrum IP exploration method. This method uses pseudo-random spread spectrum signals as excitation signals and employs a wireless distributed array to collect data (Yan et al., 2021). This method has the advantages of strong IP anomaly differentiation between ore and non-ore zones and strong anti-interference capabilities.

Introduction to Spread Spectrum Signals

Pseudo-random spread spectrum signals are m-sequences that contain multiple fundamental frequency signals (Chun et al., 2014). Their energy is mainly concentrated at the fundamental frequency points and is generally uniformly distributed. The fundamental frequency points are linearly spaced, with the number of fundamental frequencies $N = 2^{k-1}$, where k is the order of the spread spectrum wave. The fundamental frequency value f_i is calculated using the formula $f_i = f_1 \times i$, where f_1 is the frequency value of the ith fundamental frequency and f_1 is the base frequency of the spread spectrum wave.

Figure 1 shows the time series and amplitude spectrum of a commonly used 5th-order spread spectrum wave. The base frequency of the signal is

1/16 Hz, and the time series contains three periods of the spread spectrum wave. The waveform includes only two levels, -1V and 1V. The spectrum shows that the signal energy is concentrated at the linearly spaced fundamental frequency points and is generally uniformly distributed.

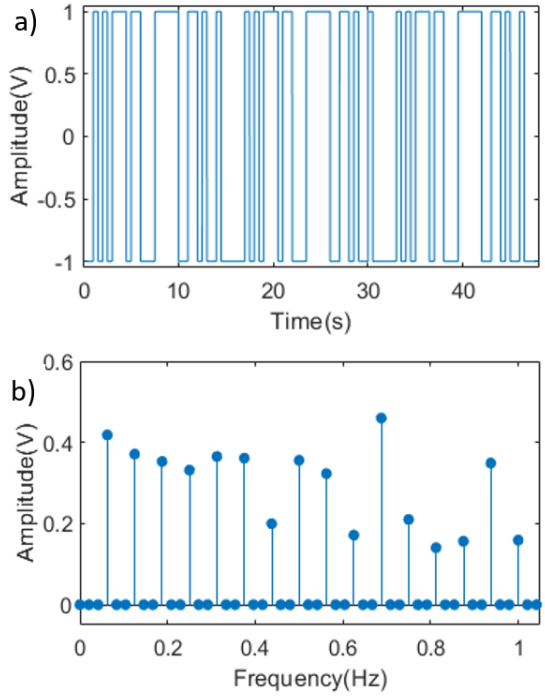

Figure 1. Waveform and amplitude spectrum of 5th order spread spectrum wave. a) Waveform, b) Amplitude spectrum

Calculation Method for Spread Spectrum Parameters

During field data collection, the control center first obtains the spread spectrum voltage signal from the acquisition station and the spread spectrum current signal from the current station in real-time via a wireless network. Then, it automatically calculates parameters such as apparent resistivity, complex resistivity phase, spread spectrum phase , and dispersion rate for each channel at each fundamental frequency. In high-interference areas, we fuse adjacent fundamental frequency signals to enhance the signal-to-noise ratio. The resulting frequency after fusion is called the composite frequency. The number of fundamental frequencies m fused for each composite frequency can be preset according to the interference situation in the work area. Generally, the greater the interference, the larger m should be. The number of composite frequencies after fusion is $N_d = \mathrm{N/m}$, where N is the total number of fundamental frequencies. Each composite frequency can yield one apparent resistivity and one complex resistivity phase, while two adjacent composite frequencies can calculate one dispersion rate and one spread spectrum phase. Thus, a single data acquisition at a survey point can simultaneously obtain N_d apparent resistivities, N_d complex resistivity phases, N_d -1 dispersion rates, and N_d -1 spread spectrum phase. The specific calculation process is as follows.

First, perform a Fourier transform on the collected spread spectrum voltage time series data and spread spectrum current time series data, and extract the spectrum values at each fundamental frequency point. Then calculate the complex resistance X_i at each fundamental frequency using the formula

$$X_i = U_i / I_i \quad (1)$$

where U_i is the spectrum value of the voltage signal at the i[th] fundamental frequency and I_i is the spectrum value of the current signal at the i[th] fundamental frequency. Then calculate the frequency value F_j of each composite frequency using the formula

$$F_j = \sum_{i=p}^{p+m-1} (w_i \times f_i), \quad (2)$$

where p is the index of the starting fundamental frequency $p = (j-1) \times m + 1$, w_i is the weighting value of the i[th] frequency (Typically taken as $\frac{1}{m}$), and f_i is the frequency value of the i[th] fundamental frequency. The complex resistance C_j of each composite frequency is calculated using the formula

$$C_j = \sum_{i=p}^{p+m-1} (w_i \times X_i) \quad (3)$$

Using C_j to calculate the apparent resistivity of each composite frequency, the apparent resistivity of the j[th] composite frequency ρ_j is

$$\rho_j = k \times \left| C_j \right|, \quad (4)$$

Where k is the coefficient of the electrical exploration array(Binley et al., 2020). Using the complex resistance of adjacent composite frequencies to calculate the dispersion rate, the dispersion rate of the j[th] composite frequency fs_j is

$$fs_j = \frac{(|C_j| - |C_{j+1}|)}{|C_j|} \times 100\% \quad (5)$$

Using the complex resistivity phase of adjacent composite frequencies to calculate the spread spectrum phase, the spread spectrum phase value of the j[th] composite frequency cp_j is

$$cp_j = \left(r \times \varphi_j - p\right)/(1-r), \quad (6)$$

Where φ_j is the complex resistivity phase of the j[th] composite frequency, and r is the frequency ratio of the composite frequencies, expressed as

$$r = F_{j+1}/F_j, \quad (7)$$

Where p is the phase correction of φ_{j+1} with respect to φ_j, expressed as

$$p = \begin{cases} \varphi_{j+1}, \left(\varphi_j - \pi \le \varphi_{j+1} \le \varphi_j + \pi\right) \\ \varphi_{j+1} - 2\pi, \left(\varphi_{j+1} > \varphi_j + \pi\right) \\ \varphi_{j+1} + 2\pi, \left(\varphi_{j+1} < \varphi_j - \pi\right) \end{cases} \quad (8)$$

By this method, multiple composite frequencies' apparent resistivities, complex

resistivity phases, spread spectrum phase and dispersion rates can be obtained. Analyzing the variation of these parameters in the frequency domain allows for the differentiation of IP anomalies between ore and non-ore zones. Increasing the number of fundamental frequencies m fused can improve the signal-to-noise ratio and enhance the system's anti-interference capability, while decreasing m can improve the resolution of each parameter in the frequency domain and enhance the ability to differentiate IP anomalies between ore and non-ore zones.

Processing of Measured Data

Based on the proposed spread spectrum IP parameter calculation method, we processed and verified the anti-interference capability of multi-frequency fusion using field test data. The test setup used an array four-electrode sounding array, with a profile length of 1800m, a survey point spacing of 40m, and 46 survey points. The coordinates of the receiving electrodes ranged from -20m to 1820m, and the power supply points A and B were located at 880m and 960m, respectively. A 5th-order spread spectrum wave with a frequency of 0.0625Hz was transmitted from AB, with a current of 0.5A. All survey points were sampled synchronously at a rate of 15Hz for 96 seconds, covering six signal periods. The varying distances of the survey points from the power supply points result in different received signal strengths. Consequently, the signal-to-noise ratios (SNR) of the collected data also vary. The farther a survey point is from the power supply point, the weaker its SNR.

To evaluate data quality, we typically divide the time series into multiple segments, calculate the IP parameters for each segment, and then average all segment parameters as the estimated IP parameter. The mean square error of all segment parameters is calculated as the estimation error. For this test, we used a 32-second segment duration and divided the data into three segments. The mean and mean square error of the three segments' results were calculated, with the mean serving as the final result and the mean square error as the estimation error to assess result quality. We first selected data from survey points 1 and 12 for calculation. Survey point 1 is located at the center coordinate of 0m, 880m from the A power supply point, with a low SNR. Survey point 12 is located at the center coordinate of 440m, 40m from the A power supply point, with a high signal-to-noise ratio (SNR). Figure 2 shows the apparent resistivity and complex resistivity phase at survey points 1 and 12 under single frequency non-fusion and 4-frequency fusion conditions. The figure shows that the data quality at survey point 1 is poor. Without frequency fusion, the error bars for the apparent resistivity and phase are large, and their trends with frequency are not apparent. However, after frequency fusion, the data quality of both parameters significantly improves, the error bars are reduced, and the trends become more evident. The data quality at survey point 12 is good; without frequency fusion, the apparent resistivity and phase show a clear trend with frequency, although some frequency points have larger errors. After frequency fusion, the error bars for the data significantly reduce, but the frequency resolution also decreases.

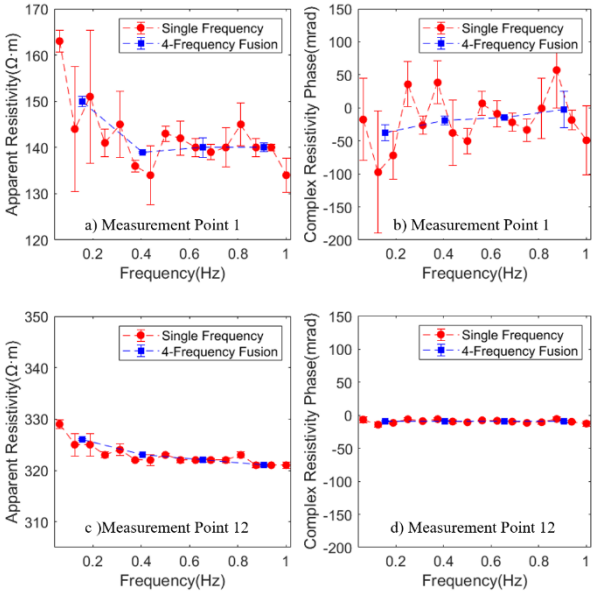

Figure 2. Processing Results at Survey Points 1 and 12 for Single Frequency Non-Fusion and 4-Frequency Fusion

To further compare the calculation results of single frequency and multi-frequency fusion, we calculated the IP parameters for all survey points along the entire profile. The results for the first frequency point are shown in Figure 3. The figure shows that in the middle section of the profile, where the SNR is strong, the error bars for all parameters are small, and the results of single frequency non-fusion and 4-frequency fusion calculations are almost identical. In the sections at both ends of the profile, where the SNR is poor, the parameters after 4-frequency fusion are smoother and have smaller error bars than those obtained from single frequency non-fusion.

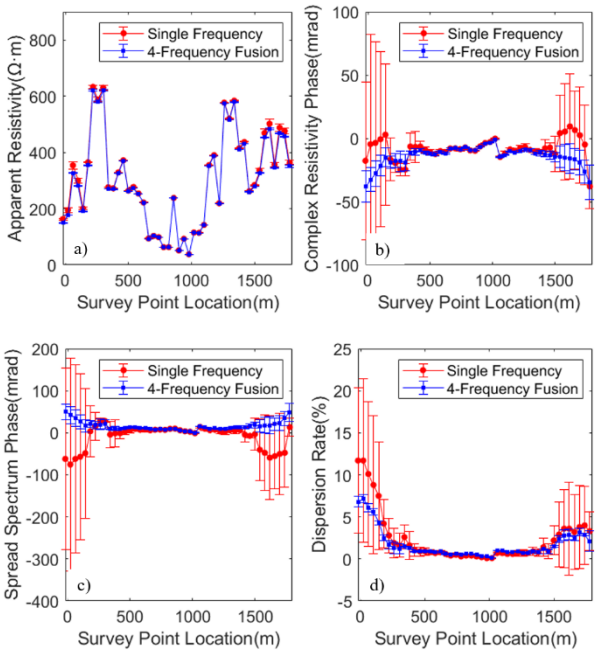

Figure 3. Processing Results for the First Frequency Point across the Entire Profile for Single Frequency Non-Fusion and 4-Frequency Fusion

Conclusion

In order to distinguish between ore and non-ore IP anomalies and to improve the anti-interference capability of the IP method, we introduced pseudo-random spread spectrum signals into IP exploration and achieved multi-frequency and multi-parameter calculations for SSIP. Using frequency fusion methods, we improved the signal-to-noise ratio (SNR) of the data and processed field-measured data. The results show that frequency fusion can enhance the anti-interference capability of SSIP. This method can be adapted to different levels of interference in the work area. In non-interference zones, single-frequency complex resistivity can be used directly to calculate IP parameters and distinguish between ore and non-ore IP anomalies based on the trends of these parameters. In high-interference zones, frequency fusion can be used to calculate IP parameters at composite frequencies, thereby improving the anti-interference capability of the IP parameters.

Acknowledgements

We would like to extend our special thanks to Giant Sequoia Artificial Intelligence Technology (Changsha) Co., Ltd. for providing the instruments and data for this research.

References

Binley, A., & Slater, L. (2020). Resistivity and Induced Polarization: Theory and Applications to the Near-Surface Earth. Cambridge University Press. https://doi.org/10.1017/9781108685955

Cen, W., & Li, Z. (2023, August). A noise reduction method based on PSR-fastICA for spectrum-induced polarization data. In Second International Conference on Electronic Information Technology (EIT 2023) (Vol. 12719, pp. 50-56). SPIE.

Chun Shaoheng, Chen Rujun, & Gen Minghui. (2014). Pseudo-random sequence and its progress in electrical prospecting applications. Progress in Geophysics, 29(1).

Guo, Z., Xue, G., Liu, J., & Wu, X. (2020). Electromagnetic methods for mineral exploration in China: A review. *Ore Geology Reviews*, *118*, 103357.

Liu, W., LÜ, Q., Lin, P., & Chen, R. (2019). Anti-interference processing of multi-period full-waveform induced polarization data and its application to large-scale exploration. Chinese Journal of Geophysics, 62(10), 3934-3949.

Okada, K. (2022). Breakthrough technologies for mineral exploration. Mineral Economics, 35(3), 429-454.

Revil, A., Vaudelet, P., Su, Z., & Chen, R. (2022). Induced polarization as a tool to assess mineral deposits: A review. Minerals, 12(5), 571.

Su, Z., Revil, A., Ghorbani, A., Zhang, X., Zhao, X., & Richard, J. (2023). Combining electrical resistivity, induced polarization, and self-potential for a better detection of ore bodies. Minerals, 14(1), 12.

Yan chao, Chen Rujun, Shen Ruijie, Wu Xilin, Wang Xiaojie, Chen Xingsheng, & Liu Haifei. (2021). Distributed multi-channel synchronous data acquisition system for electrical and electromagnetic methods. Progress in Geophysics, 36(4), 1743-1750.